Journal of Integrative Medicine 22 (2024) 493–502

Contents lists available at ScienceDirect

Journal of Integrative Medicine

journal homepage: www.jcimjournal.com/jim
www.journals.elsevier.com/journal-of-integrative-medicine

Original Research Article

Berberine alleviates ovarian tissue damage in mice with hepatolenticular degeneration by suppressing ferroptosis and endoplasmic reticulum stress

Qian-zhuo Liu [a], Hui Han [a,*], Xin-ru Fang [a], Lu-yao Wang [a], Dan Zhao [a], Miao-zhu Yin [a], Nian Zhang [a], Peng-yu Jiang [a], Zhi-hui Ji [a], Li-min Wu [b,*]

[a] *Department of Neurology, the First Affiliated Hospital of Anhui University of Chinese Medicine, Hefei 230031, Anhui Province, China*
[b] *Center for Reproduction and Genetics, the First Affiliated Hospital of USTC, Division of Life Sciences and Medicine, University of Science and Technology of China, Hefei 230031, Anhui Province, China*

ARTICLE INFO

Article history:
Received 2 January 2024
Accepted 15 April 2024
Available online 23 May 2024

Keywords:
Berberine
Hepatolenticular degeneration
Copper deposition
Ferroptosis
Endoplasmic reticulum stress

ABSTRACT

Objective: Hepatolenticular degeneration (HLD) is an autosomal recessive disorder that manifests as multiorgan damage due to impaired copper (Cu) metabolism. Female patients with HLD often experience reproductive impairments. This study investigated the protective effect of berberine against ovarian damage in toxic-milk (TX) mice, a murine model for HLD.
Methods: Mice were categorized into control group, HLD TX group (HLD group), penicillamine (Cu chelator)-treated TX group and berberine-treated TX group. Body weight, ovary weight and the number of ovulated eggs were recorded. Follicular morphology and cellular ultrastructure were examined. Total iron, ferrous iron (Fe^{2+}) and trivalent iron (Fe^{3+}) levels, as well as malondialdehyde (MDA), glutathione (GSH) and oxidized glutathione (GSSG), were measured in the ovaries. Western blot analysis was used to analyze the expression of proteins related to ferroptosis and endoplasmic reticulum (ER) stress.
Results: Ovarian tissue damage was evident in the HLD group, with a significant increase in ferroptosis and ER stress compared to the control group. This damage was inhibited by treatment with penicillamine, a Cu chelator. Compared with the HLD group, berberine increased the number of ovulations, and improved ovarian morphology and ultrastructure. Further, we found that berberine reduced total iron, Fe^{2+}, MDA and GSSG levels, elevated GSH levels, decreased the expression of the ferroptosis marker protein prostaglandin-endoperoxide synthase 2 (PTGS2), and increased glutathione peroxidase 4 (GPX4) expression. Furthermore, berberine inhibited the expression of ER stress-associated proteins mediated by the protein kinase RNA-like ER kinase (PERK) pathway.
Conclusion: Ferroptosis and ER stress are involved in Cu-induced ovarian damage in TX mice. Berberine ameliorates ovarian damage in HLD TX mice by inhibiting ferroptosis and ER stress.
Please cite this article as: Liu QZ, Han H, Fang XR, Wang LY, Zhao D, Yin MZ, Zhang N, Jiang PY, Ji ZH, Wu LM. Berberine alleviates ovarian tissue damage in mice with hepatolenticular degeneration by suppressing ferroptosis and endoplasmic reticulum stress. *J Integr Med*. 2024; 22(4): 493–502.

1. Introduction

Hepatolenticular degeneration (HLD) is an autosomal recessive disorder caused by mutations in *ATP7B* gene [1]. Patients with impaired copper (Cu) metabolism and excessive Cu deposition in the liver, brain, kidneys and cornea often exhibit symptoms of liver disease, neurological disorders, kidney damage and corneal pigment rings [2]. Furthermore, numerous case reports document the combination of HLD with reproductive damage. Female patients with HLD often experience irregular menstruation, amenorrhea and spontaneous abortion [3–5]. Therefore, paying attention to reproductive impairments in patients with HLD is crucial.

* Corresponding authors.
E-mail addresses: hanhuidoctor2022@163.com (H. Han), wlm@ustc.edu.cn (L.M. Wu).

https://doi.org/10.1016/j.joim.2024.05.003

Ferroptosis is a form of iron-dependent regulatory cell death caused by massive lipid peroxide-mediated membrane damage. Ferroptosis is associated with various female reproductive disorders, including polycystic ovary syndrome, ovarian insufficiency, and spontaneous abortion [6]. Additionally, Cu can play an unfavorable role by inducing the onset of ferroptosis [7]. Recent studies have shown that ferroptosis is involved in HLD [8], and conditions such as iron overload [9] and oxidative/antioxidative imbalance [10] are also present in HLD organisms. Therefore, ferroptosis modulation may be an effective means of alleviating and treating HLD. Endoplasmic reticulum (ER) stress is a protective response, but sustained ER stress can result in cell death [11,12]. Excessive ER stress has been found to negatively affect oocyte development and induce reproductive disorders [13]. ER stress is strongly associated with ferroptosis [14,15]. Cu-induced toxicity is closely related to ER stress [16]. However, whether ferroptosis and ER stress are involved in ovarian damage induced by Cu exposure in patients with HLD remains unknown.

Berberine, an alkaloid extracted from the traditional Chinese medicine, Rhizoma Coptidis, exhibits anti-inflammatory, antioxidant, neuroprotective and other pharmacological effects [17].

Berberine also enhances ovarian function in mice with premature ovarian failure by reducing oxidative stress and maintaining normal ovarian hormone levels [18,19]. In addition, berberine has a proven safety profile in the treatment of ovarian diseases. For example, berberine increased cell viability of ovarian granulosa cells in rats with premature ovarian failure [18]. Berberine improves ovulation rates in patients with polycystic ovary syndrome and can be used in premenopausal women who want to get pregnant, with virtually no side effects [20]. Another controlled, randomised, multi-centre clinical trial found that berberine improved menstrual status, hormone levels and ovarian structure in patients with polycystic ovary syndrome, without specific side effects [21]. Recent studies have demonstrated that berberine reduced the accumulation of intracellular reactive oxygen species (ROS) and iron deposition [22,23]. Additionally, berberine attenuated cognitive deficits in a mouse model of Alzheimer's disease by inhibiting ER stress mediated by the protein kinase RNA-like ER kinase (PERK) pathway [24]. These findings prompted us to investigate the protective effects of berberine against HLD Cu deposition-induced ovarian damage and its relationship with ferroptosis and ER stress.

In this study, we used HLD toxic-milk (TX) model mice for in vivo experiments to investigate the protective effect of berberine against ovarian damage in TX mice and its potential mechanism of action. We discovered that impaired Cu metabolism in TX mice can cause ovarian damage by inducing ferroptosis and ER stress, and that berberine can inhibit this injurious process. These findings offer supportive evidence for the clinical application of berberine as a potential agent for treating ovarian impairment in patients with HLD.

2. Materials and methods

2.1. Experimental animals

Thirty female TX mice (C3He-*ATP7B*$^{\text{tx-j}}$) carrying an *ATP7B* gene mutation (Jackson Laboratory Animal Center, USA), aged 8–10 weeks and weighing 18–20 g, were divided into HLD, penicillamine, and berberine groups, each consisting of 10 mice, using a random number table. The control group comprised homozygous control DL-strain mice of TX mice, with 10 mice. All groups of mice were housed in a specific pathogen-free laboratory under a 12-hour light and 12-hour dark cycle. The temperature of the animal room was 19–21 °C, with humidity levels between 50% and 60%, and the mice had *ad libitum* access to food and water. All animal experiments were approved by the Animal Experiment Ethics Committee of Anhui University of Traditional Chinese Medicine (approval number: 2014019).

2.2. Drug administration and sampling

Berberine was purchased from Sigma-Aldrich (CAS: 633-65-8, MO, USA), and penicillamine was obtained from Sine (NDC: H31022286, Shanghai, China). The mice were acclimatized and fed for 1 week before treatment commencement. In the berberine group, mice were gavaged with 0.15 g/(kg·d) [19], in the penicillamine group, mice were gavaged with 0.1 g/(kg·d), and in the HLD group and control group, mice were gavaged with an equal volume of saline. All 4 groups of mice were gavaged at the same time in the morning once per day for 3 weeks. Between 9:00 and 11:00 a.m., the day after gavage, all 4 groups of mice were injected intraperitoneally with 10 IU of pregnant mare serum gonadotropin (PMSG). After 24 h, 4 mice from each group were anesthetized by injecting 1% sodium pentobarbital (50 mg/kg). The left ovary was collected and preserved in formaldehyde for hematoxylin and eosin (HE) staining, whereas the right ovary tissue was placed in glutaraldehyde solution for transmission electron microscopy (TEM). At 48 h after PMSG injection, the remaining 6 mice in each group were intraperitoneally administered 10 IU of human chorionic gonadotropin (HCG). After 14 h, each mouse was anesthetized by intraperitoneal injection of sodium pentobarbital. Subsequently, the mice were euthanized by cervical dislocation, and all eggs discharged from both ovaries were removed from the oviduct ampulla and counted under a microscope. Ovarian tissues were stored at −80 °C for Western blot (WB) and biochemical assays.

2.3. Calculation of the number of ovulations

A 1 mL syringe needle was used to puncture the oviduct ampulla, causing the expulsion of follicles. The number of eggs discharged by each mouse was counted using an inverted optical microscope (Olympus, CKX31, Japan) [25].

2.4. Assessment of the ovarian coefficient

All mice were weighed before administering anesthesia. Subsequent to anesthesia, both ovaries were extracted, washed in saline, blotted on filter paper, and then weighed. The ovarian coefficient = bilateral ovarian weight (g)/mouse weight (g) × 100% [26].

2.5. Histological analysis

Ovarian tissues from each group were fixed with 4% paraformaldehyde, and paraffin sections were prepared. Sections were baked at 64 °C for 1 h. Sections were stained with HE (B006, B005, ebiogo, Hefei, China) and images were captured using an optical microscope (Olympus, CX41, Japan). The structural and follicular development of mouse ovarian tissue was observed, and the number of follicles in each developmental period was quantified in the section with the largest diameter.

2.6. Observation of the ultrastructure of ovarian cells by TEM

A 1 mm^3 block of ovarian tissue was taken. Ovary tissues were fixed sequentially with 2.5% glutaraldehyde (18426, TED PELLA, INC, Beijing, China) and post-fixed in 1% osmium tetroxide (18456, TED PELLA INC, Beijing, China). The prepared tissues were dehydrated using a graded series of ethanol and acetone. Next, the tissue was embedded in epoxy resin, and ultrathin sections were prepared and stained with uranium acetate-lead citrate. Finally, changes in the ultrastructure of the ovarian tissue cells were observed using TEM (JEM1400, JEOL, Japan).

2.7. Determination of iron content

The iron concentration in the ovarian tissue was measured using an iron assay kit (I291, Tohito Chemical Technology Co., Shanghai, China). Ovarian tissues (10 mg) were rapidly homogenized in iron assay buffer. Subsequently, the insoluble material was removed via centrifugation at 16,000*g* for 10 min. The supernatant (400 μL) was taken, and 100 μL was added to each tube to create the ferrous iron (Fe^{2+}) sample, total iron sample, and blank sample. Reducer solution (20 μL) was added to the standard tube, and 20 μL of assay buffer was added to the Fe^{2+} tube. Additionally, 20 μL of reducer solution was added to the total iron sample tube, and 20 μL of assay buffer was added to the sample blank tube. All standard, sample and blank tubes were incubated at 37 °C for 15 min. The absorbance was measured at 593 nm [27]. Finally, the data were copied to a table and the Fe^{2+} and trivalent iron (Fe^{3+}) concentrations were automatically calculated.

2.8. Determination of malondialdehyde, glutathione and oxidized glutathione levels in ovarian tissue

Ovarian tissue was removed from a −80 °C freezer and thawed in an ice water bath. Levels of malondialdehyde (MDA), glutathione (GSH) and oxidized glutathione (GSSG) in ovarian tissues were determined using the corresponding kits (A003-1, A006-2 and A061-1, Nanjing Jiancheng Bioengineering Institute, China), following the manufacturer's instructions. MDA levels in ovarian tissues were measured using the thiobarbituric acid method [28], and GSH and GSSG levels in ovarian tissues were measured using a microplate method and a microenzymatic assay, respectively. GSH can react with 5,5′-dithiobis-(2-nitrobenzoic acid) (DTNB) to produce a yellow compound that can be quantified at 405 nm. The amount of GSSG in tissues was determined using the cyclic reaction of DTNB.

2.9. Detection of ferroptosis and ER stress-related proteins using Western blot

Ovarian tissue samples were homogenized on ice using the preconfigured radio immunoprecipitation assay solution. The homogenate was transferred to a centrifuge tube, and the supernatant was used as the total protein extract. The protein content was determined using the bicinchoninic acid assay method. Sodium dodecyl sulfate–polyacrylamide gel electrophoresis (SDS-PAGE) (10%) was used to separate the proteins based on their molecular weight, and the resulting bands were transferred to a membrane. The polyvinylidene fluoride (PVDF) membrane was blotted with 5% skim milk for 2 h. The membrane was then incubated overnight at 4 °C with the primary antibodies against prostaglandin-endoperoxide synthase 2 (PTGS2) (ab255420, 1:000, Abcam, Cambridge, UK), glutathione peroxidase 4 (GPX4) (bs-3884R, 1:1000, Bioss, Beijing, China), glucose-regulated protein 78 (GRP78) (bs-1219R, 1:1000, Bioss), PERK (3192S, 1:1000, CST, Boston, USA), p-PERK (3179S, 1:1000, CST), α subunit of eukaryotic initiation factor 2 (eIF2α) (5324S, 1:1000, CST), p-eIF2α (bs-14541R, 1:1000, Bioss), activating transcription factor 4 (ATF4) (bs-1531R, 1:1000, Bioss) and C/EBP homologous protein (CHOP) (BS1136, 1:5000, Bioworld, Nanjing, China). The next day, the PVDF membrane was rinsed thrice in Tris-buffered saline with Tween 20 (TBST) and then incubated with the secondary goat anti-rabbit IgG antibody (ZB-2301, 1:20,000, Zsbio, China) for 2 h and rinsed thrice in TBST. Finally, an enhanced chemiluminescence developer was added for protein detection. The gray value of each band was quantified using ImageJ software to determine relative abundance of the detected proteins.

2.10. Statistical analysis

All the statistical analyses were conducted using Statistical Product and Service Solutions version 23.0 (IBM Corporation, NY, USA). GraphPad Prism version 9.5 (San Diego, CA, USA) was used to prepare plots. There were no data points in the experimental data that were significantly outside of reasonable ranges, so no data points were excluded from this study. In this study, we used mean ± standard deviation to represent the data in the graphs. Comparisons between multiple groups were performed using a one-way analysis of variance. Post hoc multiple comparisons were performed using least significant difference when variances were equal, and Tamhane's T2 was used when variances were not equal. $P < 0.05$ was considered statistically significant.

3. Results

3.1. Effects of berberine on body weight, ovarian weight and ovarian coefficient in TX mice

Table 1 shows the body weight, organ weight and organ coefficient ratio for each group of mice, which are essential indicators for assessing the body and organ state. The findings revealed that mouse body weight and ovary coefficient were lower in the HLD TX group (HLD group) than in the control group, but the difference was not statistically significant. However, ovary weights were significantly reduced in the HLD group of mice compared with the controls ($P < 0.01$). In comparison with the HLD group, mice in the penicillamine group exhibited a significantly higher ovary weight ($P < 0.05$), whereas no significant differences were observed in mouse body weight and ovary coefficient. The berberine group did not show significant elevation in body weight, ovarian weight or ovarian coefficient compared with the HLD group. No significant differences were observed between the berberine and penicillamine groups. Fig. 1 displays the measurement of ovaries of each group of mice.

3.2. Effects of berberine on the number of eggs released

The extent of ovulation serves as an indicator of ovarian function. To evaluate the impact of Cu on ovulation and the protective influence of berberine on ovarian function in TX mice, we implemented an ovulation promotion protocol involving 10 IU PMSG + 10 IU HCG. The results revealed a significantly lower number of ovulations in the HLD group than in the control group ($P < 0.001$), indicating that Cu deposition inhibited ovarian function in mice. The deleterious effect of Cu on ovarian function was mitigated by the Cu chelator penicillamine, as evidenced by a significant increase in ovulation in TX mice ($P < 0.01$). Moreover, TX mice exhibited a significantly higher number of ovulations after treatment with berberine than those in the HLD group ($P < 0.05$). No significant differences were observed between the berberine and penicillamine groups (Table 2).

3.3. Effects of berberine on the morphology of ovary tissues

To assess the impact of berberine on the ovarian morphology of TX mice, we conducted HE staining of mouse ovarian tissue (Fig. 2). In the control group (Fig. 2A, B), normally developed follicles were observed at all levels, and were characterized by rounded oocytes and well-arranged granulosa cells encircling them. Follicle development in the HLD group, however, was typified by nuclear

Table 1
Comparison of body weight, ovarian weight and ovarian coefficient ratio of mice in different groups.

Group	*n*	Body weight (g)	Ovarian weight (g)	Ovarian coefficient ratio (%)
Control	10	24.48 ± 1.07	0.022 ± 0.003	0.090 ± 0.012
HLD	10	23.33 ± 1.63	0.019 ± 0.003**	0.080 ± 0.014
Penicillamine	10	24.26 ± 0.80	0.021 ± 0.002#	0.089 ± 0.010
Berberine	10	24.27 ± 0.81	0.021 ± 0.003	0.085 ± 0.013

**$P < 0.01$, compared with the control group; #$P < 0.05$, compared with the HLD group. HLD: hepatolenticular degeneration.

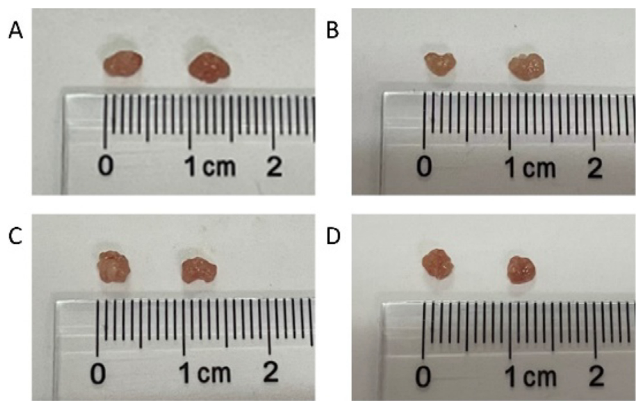

Fig. 1. Images of the ovaries from four mouse groups. A: control group; B: hepatolenticular degeneration group; C: penicillamine group; D: berberine group.

Table 2
Average number of eggs released after HCG administration in mice across different groups.

Group	*n*	Eggs released after HCG administration
Control	6	45.83 ± 7.78
HLD	6	31.83 ± 2.86***
Penicillamine	6	40.00 ± 3.63##
Berberine	6	39.17 ± 3.66#

***$P < 0.001$, compared with the control group; #$P < 0.05$, ##$P < 0.01$, compared with the HLD group. HCG: human chorionic gonadotropin; HLD: hepatolenticular degeneration.

condensation of the oocyte, collapse and breakage of the zona pellucida, and an increase in atretic follicles, indicating severe impairment of follicle morphology due to Cu deposition in TX mice (Fig. 2C, D). In mice treated with penicillamine, follicular morphology was more normal, and the number of atretic follicles was decreased compared to the HLD group (Fig. 2E, F), providing further evidence of the detrimental effect of Cu on the ovary. The berberine group (Fig. 2G, H) exhibited normally developed secondary and antral follicles, with tightly arranged granulosa cells, and follicular morphology closely resembled that of the control group. Berberine treatment appeared to improve follicular morphology.

Follicular development occurs in four stages: primordial, primary, secondary and antral. When an abnormality exists at any stage of follicular development, the follicle shrinks and degenerates, forming an atretic follicle. Here, we counted primary, secondary, antral and atretic follicles in HE sections of the ovaries of TX mice. The results showed a significant decrease in the number of secondary and antral follicles and a significant increase in atretic follicles in the HLD group compared with the control group ($P < 0.05$). The numbers of secondary ($P < 0.01$) and antral ($P < 0.05$) follicles were significantly higher in the penicillamine group than in the HLD group. This suggests that Cu contributes to the inhibition of follicular development and maturation, and this inhibition is attenuated by chelating Cu. Compared with the HLD group, mice treated with berberine displayed a significant increase in the number of secondary and antral follicles ($P < 0.05$) and a decrease in the number of atretic follicles ($P < 0.05$). This suggests that berberine promoted follicular development and maturation in TX mice (Fig. 3).

3.4. Impact of berberine on the ultrastructure of mouse ovary

Mitochondrial dysfunction and increased ROS generation are the major features of ferroptosis. Therefore, we examined mitochondrial morphology in the ovarian tissues of TX mice. TEM observations revealed distinct mitochondrial alterations in the HLD group, including a reduced mitochondrial number, evident swelling, an increase in vacuolar mitochondria, and a reduction or disappearance of mitochondrial cristae (Fig. 4B). Moreover, the HLD group exhibited a higher occurrence of mitochondria displaying specific ferroptosis-like features, such as a smaller size, increased membrane density, and the absence of mitochondrial cristae [29,30], whereas such ferroptosis-like mitochondria were rare in the other groups. In comparison with the HLD group, the mitochondrial structure was significantly improved in the berberine and penicillamine groups, and the morphology resembled that of the control group (Fig. 4C, D). Additionally, we statistically analyzed abnormally swollen mitochondria. The ratio of swollen mitochondria to total mitochondria was significantly increased in the HLD group compared with the control group ($P < 0.001$). The ratio of the number of swollen mitochondria to the total number of mitochondria was significantly lower in the penicillamine and berberine groups compared with the HLD group ($P < 0.001$ and $P < 0.01$). The percentage of swollen mitochondria was higher in the berberine group compared with the penicillamine group ($P < 0.05$).

3.5. Impact of berberine on iron content, and MDA, GSH and GSSG levels in ovarian tissues of TX mice

Because iron deposition, lipid peroxidation, and damage to the antioxidant system are crucial features of ferroptosis [31,32], we measured the levels of total iron, Fe^{2+}, Fe^{3+}, GSH and GSSG, as well as the lipid peroxidation product, MDA, in the ovaries employing appropriate kits. The results revealed that compared with the control group, total iron, Fe^{2+}, MDA and GSSG levels were significantly increased ($P < 0.001$), and GSH levels and the GSH/GSSG ratio were significantly decreased ($P < 0.001$) in the HLD group. These changes were suppressed following the chelation of Cu with penicillamine, suggesting that Cu-induced ovarian damage may be linked to ferroptosis. In the berberine group, compared with the HLD group, total iron, Fe^{2+}, MDA and GSSG levels were reduced ($P < 0.001$), and GSH levels and the ratio of GSH/GSSG were elevated ($P < 0.001$). In other words, berberine demonstrated inhibition of iron deposition, lipid peroxidation, and impairment of antioxidant system in TX mice. However, the difference between the berberine and penicillamine groups did not reach statistical significance, as depicted in Fig. 5.

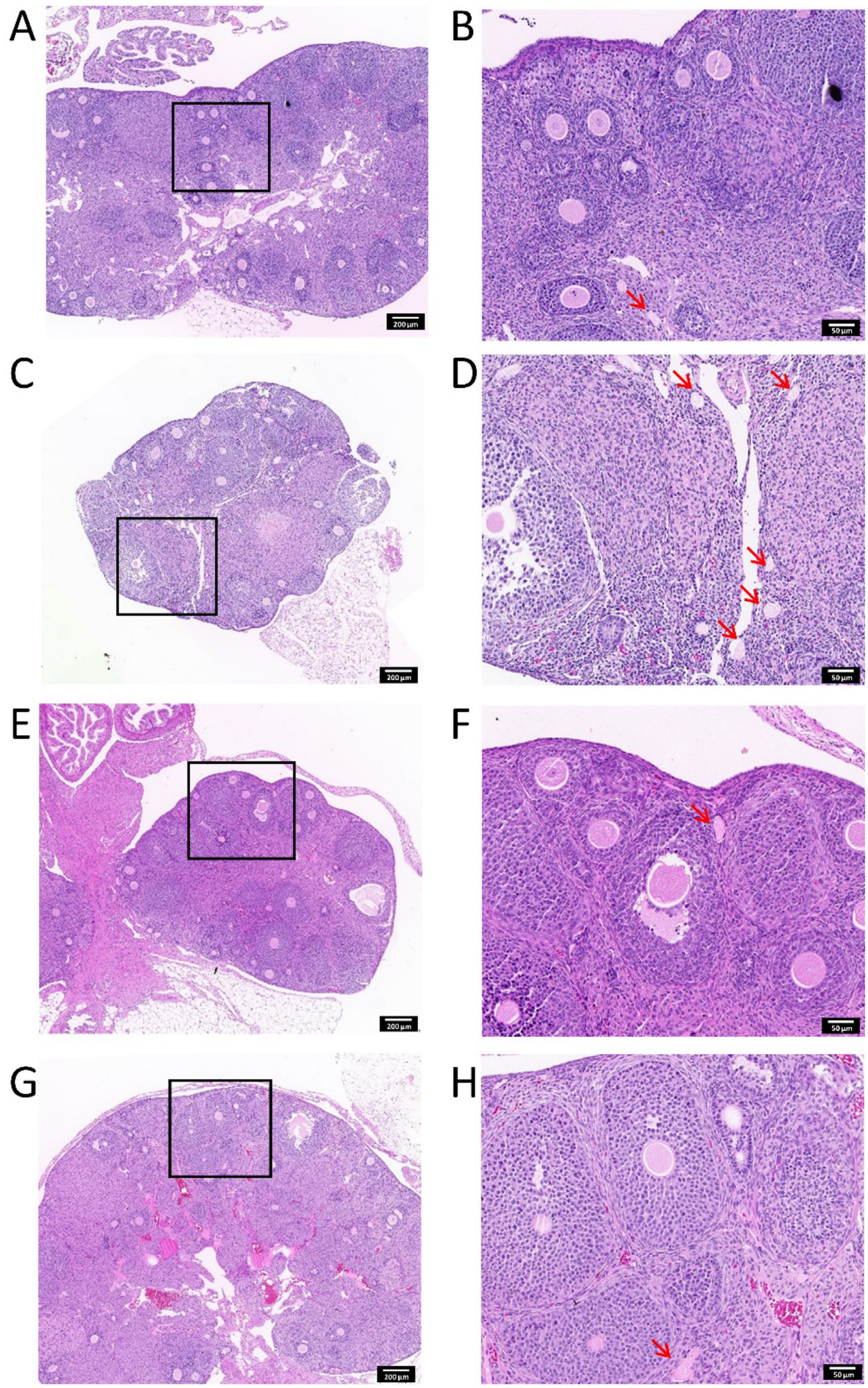

Fig. 2. Representative histopathological micrographs of mouse ovary by hematoxylin and eosin staining. A and B: control group; C and D: hepatolenticular degeneration group; E and F: penicillamine group; G and H: berberine group. Scale bar: 200 μm for A, C, E and G; 50 μm for B, D, F and H. Red arrows indicate atretic follicles.

3.6. Impact of berberine on the expression of ferroptosis-related proteins in ovarian tissues of TX mice

To further investigate the impact of ferroptosis on Cu deposition-induced ovarian injury in mice, we examined the protective effect of berberine on ovarian tissue in TX mice. We assessed the levels of PTGS2, a crucial biomarker of ferroptosis, and GPX4, an enzyme responsible for clearing lipid peroxides, in mouse ovarian tissues using WB. The results indicated that compared with the control group, PTGS2 expression was significantly upregulated and GPX4 expression was significantly downregulated in the HLD group ($P < 0.001$). After penicillamine treatment, PTGS2 expression was downregulated, and GPX4 expression was upregulated ($P < 0.001$), suggesting that inhibition of Cu deposition attenuated ferroptosis in the ovarian tissues of TX mice. In comparison with the HLD group, PTGS2 expression was downreg-

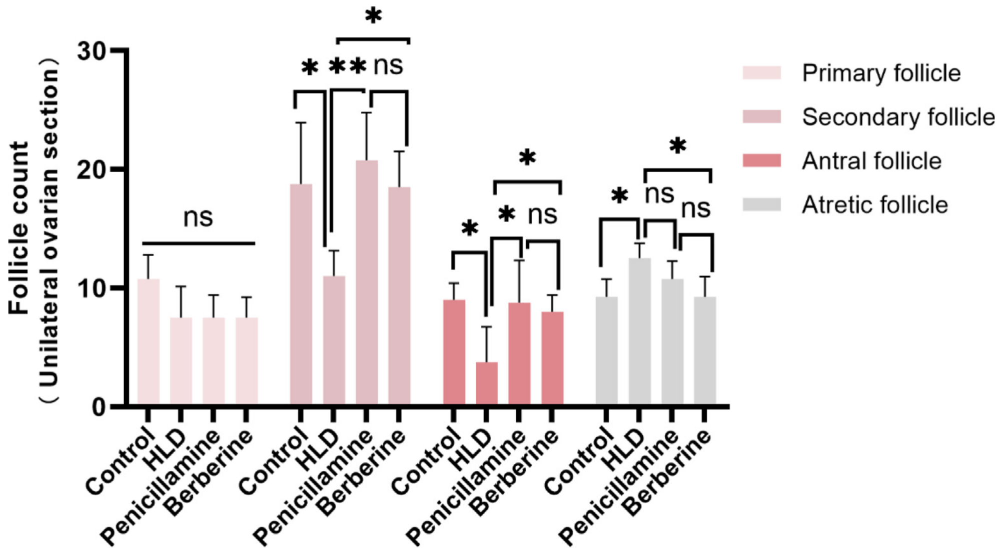

Fig. 3. Follicle counts at various levels in hematoxylin and eosin sections of the ovary (n = 4). $^{*}P$ < 0.05, $^{**}P$ < 0.01; ns: no significance. HLD: hepatolenticular degeneration.

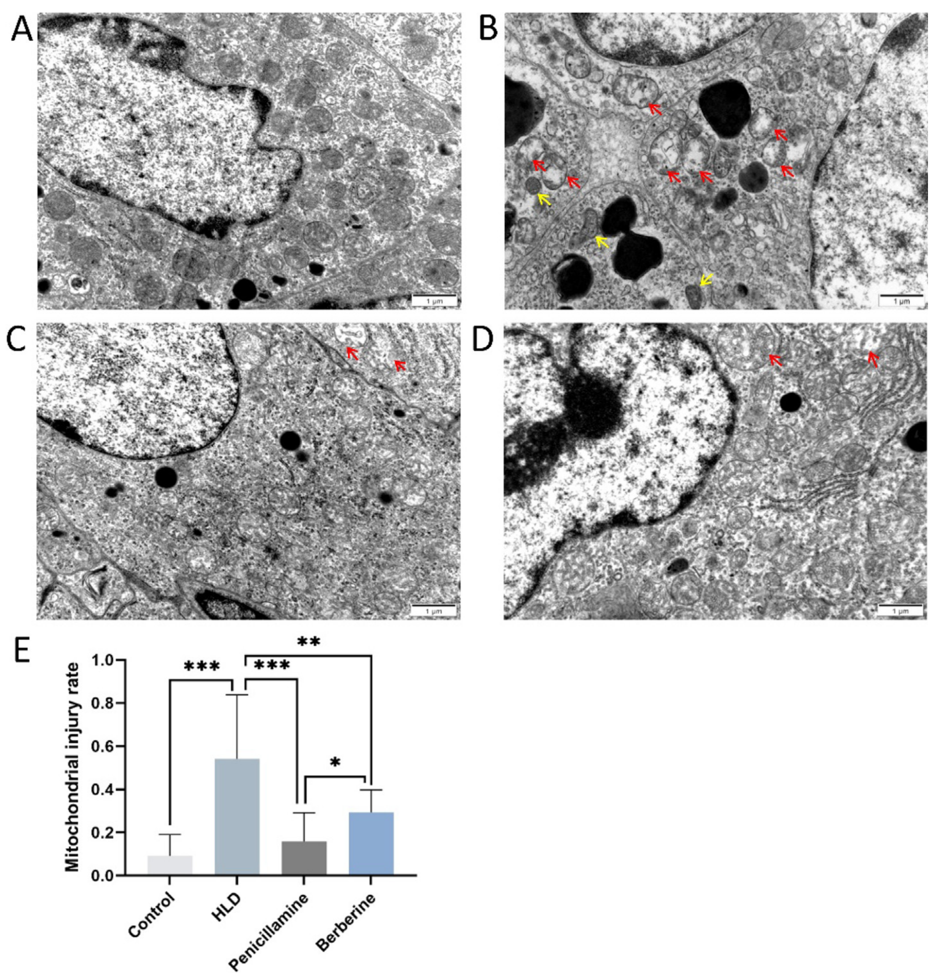

Fig. 4. Ultrastructure of mouse ovary in various groups. A: control group; B: HLD group; C: penicillamine group; D: berberine group. Scale bar: 1 μm. Red arrows point to abnormally swollen mitochondria; yellow arrows point to shrunken mitochondria. E: ratio of the number of swollen mitochondria to the total number of mitochondria (n = 4). $^{*}P$ < 0.05, $^{**}P$ < 0.01, $^{***}P$ < 0.001. HLD: hepatolenticular degeneration.

ulated (P < 0.001) and GPX4 expression was upregulated (P < 0.001) in both the berberine and penicillamine groups. This indicates that berberine inhibited ferroptosis in the ovarian tissues of TX mice. However, the difference between the penicillamine and berberine groups was not statistically significant, as illustrated in Fig. 6.

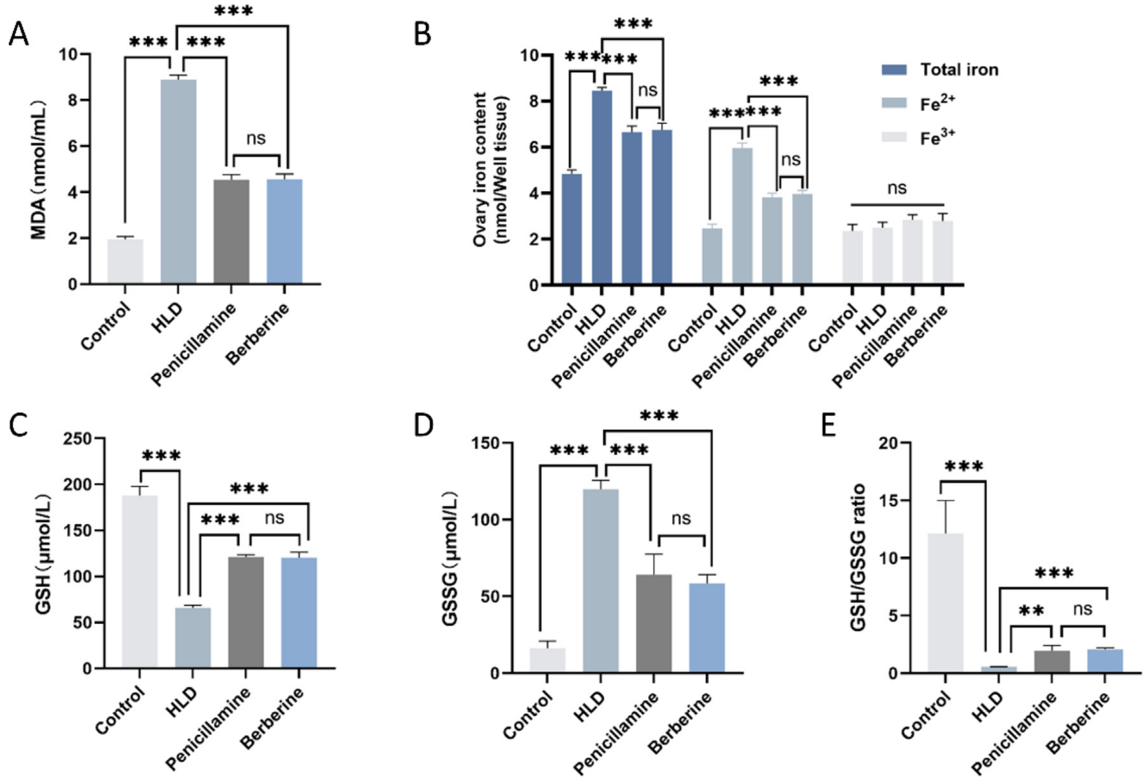

Fig. 5. MDA, total iron, Fe^{2+}, Fe^{3+}, GSH, GSSG and GSH/GSSG levels in various groups. A–E: the relative levels of MDA (A), total iron, Fe^{2+} and Fe^{3+} (B), GSH (C), GSSG (D), and GSH/GSSG (E) in ovary tissues (n = 6). $^{**}P$ < 0.01 and $^{***}P$ < 0.001; ns: no significance. Fe^{2+}: ferrous iron; Fe^{3+}: trivalent iron; GSH: glutathione; GSSG: oxidized glutathione; HLD: hepatolenticular degeneration; MDA: malondialdehyde.

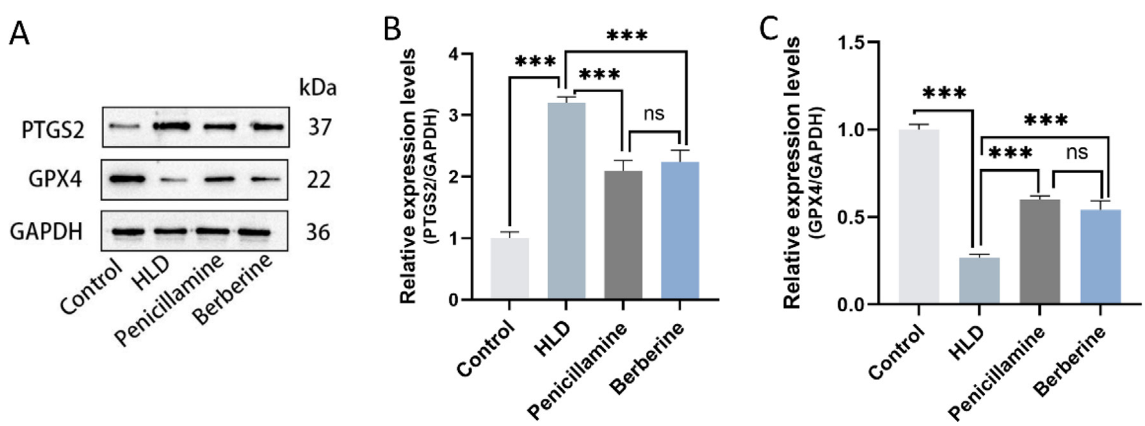

Fig. 6. Evaluation of ferroptosis-related protein expression in mouse ovary assessed by Western blot. A: PTGS2 and GPX4 protein expression. B and C: the relative intensities of PTGS2 (B) and GPX4 (C) in ovaries in different groups (n = 3). $^{***}P$ < 0.001; ns: no significance. GAPDH: glyceraldehyde-3-phosphate dehydrogenase; GPX4: glutathione peroxidase 4; HLD: hepatolenticular degeneration; PTGS2: prostaglandin-endoperoxide synthase 2.

3.7. Impact of berberine on ER stress-related protein expression in ovarian tissues of TX mice

Since ER stress mediated by the PERK pathway is closely linked to ferroptosis as well as Cu-induced cytotoxicity [33,34], we hypothesized that ER stress mediated by the PERK pathway might be implicated in Cu-induced ferroptosis, and that berberine might mitigate Cu deposition-induced ovarian damage by inhibiting ER stress. To test this hypothesis, we employed WB to examine proteins relevant to the PERK pathway. As expected, GRP78, p-PERK, p-eIF2α, ATF4 and CHOP protein expression was significantly elevated in the HLD group compared with the control group (P < 0.001), as shown in Fig. 7. After Cu chelation by penicillamine, GRP78, p-PERK, p-eIF2α, ATF4 and CHOP were significantly downregulated (P < 0.001), indicating that Cu deposition induces ER stress in the ovarian tissue of TX mice. In comparison with the HLD group, the berberine group exhibited reduced expression of GRP78, p-PERK, p-eIF2α, ATF4 and CHOP (P < 0.001, P < 0.01), suggesting that berberine could inhibit ER stress in the ovarian tissue of TX mice. However, the difference between the penicillamine and berberine groups was not statistically significant.

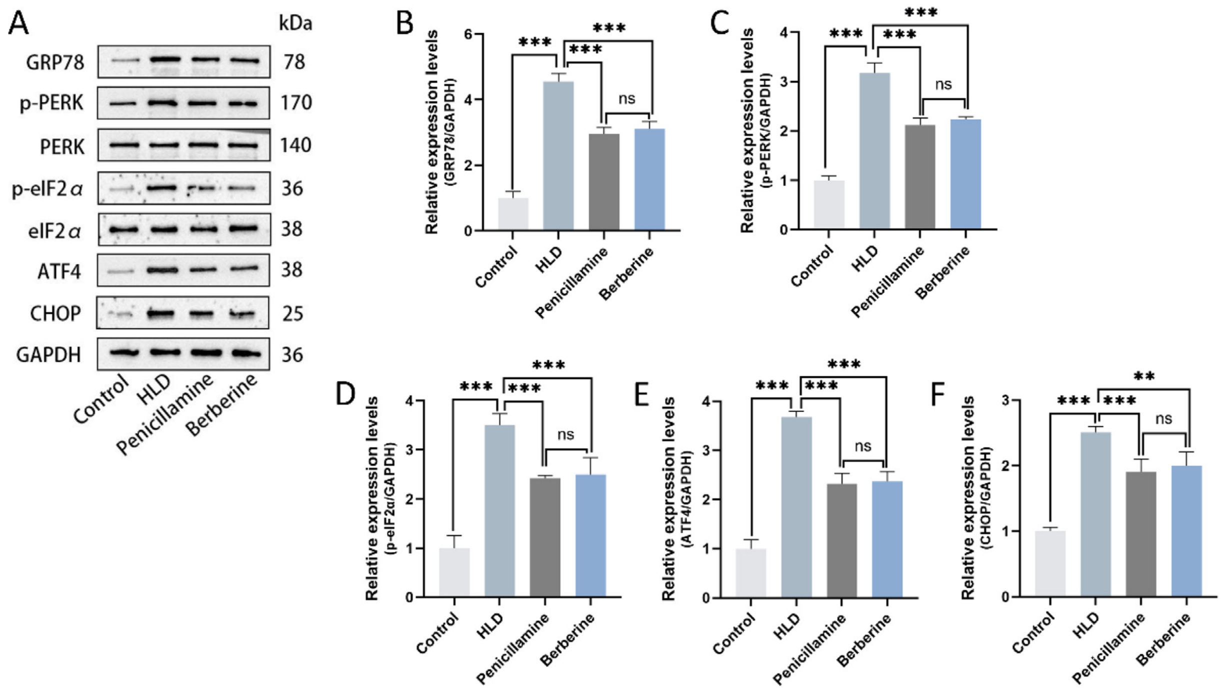

Fig. 7. ER stress-related protein expression in mouse ovary assessed by Western blot. A: GRP78, p-PERK, PERK, p-eIF2α, eIF2α, ATF4 and CHOP protein expression. B–F: the relative intensities of GRP78 (B), p-PERK (C), p-eIF2α (D), ATF4 (E) and CHOP (F) in ovaries in various groups (n = 3). $^{**}P < 0.01$, $^{***}P < 0.001$; ns: no significance. ATF4: activating transcription factor 4; CHOP: C/EBP homologous protein; eIF2α: eukaryotic initiation factor 2, α subunit; ER: endoplasmic reticulum; GAPDH: glyceraldehyde-3-phosphate dehydrogenase; GRP78: glucose-regulated protein 78; HLD: hepatolenticular degeneration; PERK: protein kinase RNA-like ER kinase.

4. Discussion

HLD is a metabolic disease characterized by aberrant function or levels of the P-type ATP7B enzyme due to genetic mutations. This leads to elevated levels of free Cu and disruptions in Cu metabolism. This, in turn, causes damage to multiple organs such as the liver and brain. Abnormalities in reproductive function are common in women with HLD. Meanwhile, several studies have reported damage to reproductive function due to Cu exposure [35]. Berberine, an alkaloid extracted from a traditional Chinese medicine, Rhizoma Coptidis, exhibits anti-inflammatory, antioxidant, neuroprotective and other pharmacological effects [17]. Liver damage is a prevalent manifestation of HLD, and berberine exerts hepatoprotective effects [36]. Furthermore, berberine has the potential to improve ovarian function in conditions such as premature ovarian failure and polycystic ovary syndrome [18,19]. Moreover, berberine has been shown to regulate iron homeostasis and lipid metabolism [22,23]. However, whether berberine ameliorates Cu deposition-induced ovarian damage in patients with HLD by inhibiting ferroptosis remains unknown.

In this experiment, we selected female TX mice deficient in the *ATP7B* gene for use as the HLD model mice [37]. We observed abnormal follicular morphology, an increase in atretic follicles, and a decrease in the number of ovulations in HLD TX mice. Elevated ovarian iron levels, reduced levels of the antioxidant GSH, elevated GSSG, and a reduction in the anti-lipid peroxidation protein GPX4 led to an increase in lipid ROS and their product MDA, inducing ferroptosis with an elevated expression of the ferroptosis signature protein, PTGS2. Additionally, we examined ER stress-related proteins that are closely linked to ferroptosis development and found that ER stress-related protein expression, mediated by the PERK pathway, was significantly upregulated. Follicular morphology and indices associated with ferroptosis and ER stress were significantly improved in mice in the berberine intervention. Impaired Cu metabolism has been shown to induce ferroptosis and ER stress, leading to ovarian tissue damage. Berberine ameliorated ovarian damage in female TX mice by inhibiting ferroptosis and ER stress (Fig. 8).

Ferroptosis is a recently identified form of cell death distinct from apoptosis and necrosis, characterized by an iron-dependent lipid peroxidation reaction [38]. Ferroptosis has been associated with various diseases and heavy metal toxicology. Recent studies have indicated that Cu plays a detrimental role by inducing ferroptosis [7]. PTGS2 serves as an important ferroptosis biomarker. GSH, a vital cellular antioxidant, plays a crucial role in eliminating lipid free radicals. The ferroptosis inducer erastin inhibits GSH synthesis by targeting solute carrier family 7 member 11 [39]. GSH plays a pivotal role in the production of GPX4, a selenoprotein responsible for preserving intracellular redox homeostasis. GPX4 achieves this by inhibiting lipid peroxidation and scavenging lipid peroxides [40]. GPX4 downregulation is often considered crucial for ferroptosis onset. Iron deposition and lipid peroxidation are important features of ferroptosis [31,32]. Ferroptosis, an iron-dependent mode of cell death, is driven by increased free Fe^{2+}, promoting lipid peroxidation via the Fenton reaction. Lipid peroxidation, resulting from an imbalance in the redox system of the organism, plays a key role in ferroptosis onset. Lipid peroxidation can induce ferroptosis by disrupting the phospholipid bilayer structure of the cell membrane or through the cytotoxic effects of its products such as MDA [41]. In this study, PTGS2 expression was significantly increased; GPX4 expression was significantly decreased; Fe^{2+}, MDA and GSSG were significantly elevated; and GSH was markedly reduced in the ovarian tissues of mice in the HLD group. After treatment with berberine and penicillamine, PTGS2 expression was downregulated; GPX4 expression was upregulated; Fe^{2+}, MDA and GSSG levels were significantly attenuated; and GSH consumption was significantly reduced. These results suggest that impaired Cu metabolism in TX mice induces the onset of ferroptosis in the ovaries, and berberine inhibits ferroptosis in ovarian tissues by attenuating iron levels, mitigating the accumulation of

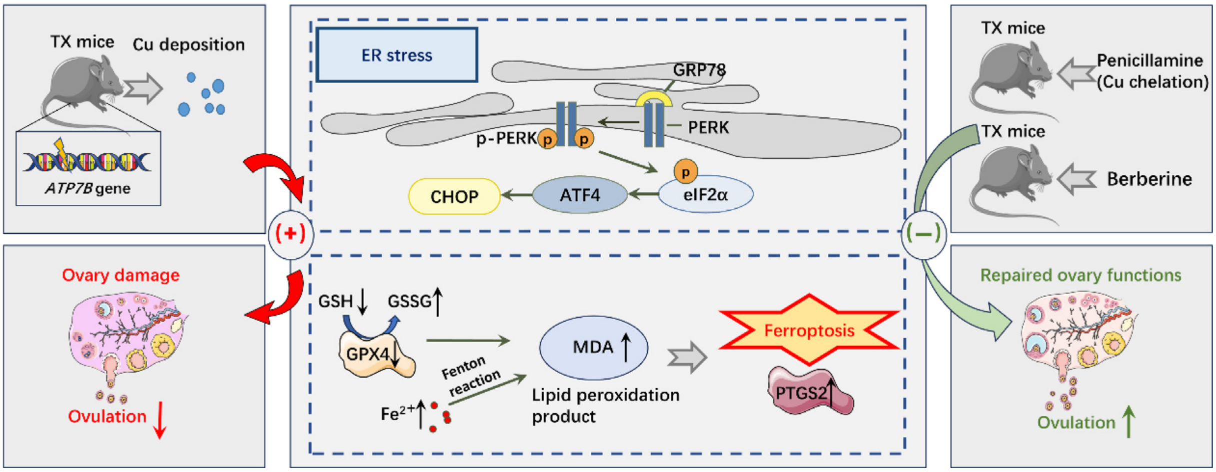

Fig. 8. Schematic diagram of the conclusion. ATF4: activating transcription factor 4; CHOP: C/EBP homologous protein; Cu: copper; eIF2α: eukaryotic initiation factor 2, α subunit; ER: endoplasmic reticulum; Fe^{2+}: ferrous iron; GPX4: glutathione peroxidase 4; GRP78: glucose-regulated protein 78; GSH: glutathione; GSSG: oxidized glutathione; MDA: malondialdehyde; PERK: protein kinase RNA-like ER kinase; p-PERK: phosphorylated PERK; PTGS2: prostaglandin-endoperoxide synthase 2; TX: toxic-milk.

lipid peroxidation products, and restoring the function of the antioxidant system in mice.

The ER stress response, initially a protective mechanism, occurs when the organism is under stress; however, it can lead to cell death if the stress is sustained or intensified. Recent studies have highlighted the close association between ER stress and ferroptosis, with increased ER stress observed during ferroptosis induced by various factors [14]. For instance, Xu et al. [42] found that ER stress is a predisposing factor for ferroptosis in colonic epithelial cells in ulcerative colitis. In a study on damage to human bronchial epithelial cells, Park et al. [43] observed that whole-cigarette smoke condensates may induce ferroptosis in bronchial epithelial cells through ER stress. PERK-mediated ER stress is strongly linked to ferroptosis, and Cu-induced cytotoxicity is associated with ER stress mediated by this pathway [34]. Under abnormal conditions, such as organismic stimulation, PERK separates from GRP78 and undergoes autophosphorylation, and activates the translation factor eIF2α, leading to upregulation of the downstream transcription factors ATF4 and CHOP [44]. Our results showed elevated expression of all relevant proteins in the PERK-mediated ER stress pathway in ovarian tissues of TX mice. Conversely, the expression of relevant proteins in the PERK-mediated ER stress pathway was downregulated following treatment with penicillamine and berberine. These findings suggest that Cu deposition in TX mice induces ER stress in the ovary, and berberine inhibits Cu-induced ER stress. This result aligns with previous studies indicating that Cu exposure can induce hepatic ER stress in yellow catfish in a time-dependent manner, resulting in the dysregulation of lipid metabolism [34].

However, this study has certain limitations. Relevant inhibitors were not employed in the in vitro cellular experiments to explore the specific link between ferroptosis and ER stress in Cu-induced ovarian damage, warranting further study. Furthermore, organs such as the liver and brain are significantly affected in patients with HLD, and the effects of berberine on liver and brain damage remain unexplored.

5. Conclusions

Our study demonstrated that disrupted Cu metabolism in TX mice can lead to ovarian tissue damage. This effect may be attributed to Cu deposition-induced ferroptosis and ER stress. Berberine exerts its protective effects by inhibiting ferroptosis and the PERK pathway-mediated ER stress. This study elucidates the mechanism by which berberine mitigates ovarian tissue damage in TX mice, a model of HLD, and provides a theoretical basis for its use in HLD treatment. Our findings offer new insights into Cu-induced ovarian tissue damage and contribute to a better understanding of Cu-associated toxicity, laying the foundation for the search for effective strategies to prevent and treat Cu-associated diseases.

CRediT authorship contribution statement

HH, WLM and LQZ designed the hypotheses and the experiments. HH, WLY and LQZ performed the experiments and their analysis. LQZ, ZD, YMZ and JPY were responsible for data collection. ZN participated in data analysis. LQZ, JZH and FXR participated in data interpretation, manuscript review and writing. LQZ was responsible for preparation of the tables and figures. All authors contributed to the scientific discussion of the data and of the manuscript.

Funding

This work was supported by the National Natural Science Foundation of China (No. 82374212, No. 81971446 and No. 81673811), the Clinical Special Translational Project of the Anhui Provincial Science and Technology Department (No. 202204295107020044) and the Key Project of the Anhui Provincial Department of Education (No. 2022AH050523).

Declaration of competing interest

The authors declare that they have no known competing financial interests or personal relationships that could have appeared to influence the work reported in this paper.

References

[1] Mulligan C, Bronstein JM. Wilson disease: an overview and approach to management. Neurol Clin 2020;38(2):417–32.
[2] Bandmann O, Weiss KH, Kaler SG. Wilson's disease and other neurological copper disorders. Lancet Neurol 2015;14(1):103–13.
[3] Rabiee A, Hamilton JPA. Pregnancy in Wilson disease. Hepatology 2018;67(4):1201–3.
[4] Reuner U, Dinger J. Pregnancy and Wilson disease: management and outcome of mother and newborns-experiences of a perinatal centre. Ann Transl Med 2019;7(Suppl 2):S56.

[5] Roseira J, Lopes R, Silva MJ, Vieira AM, Sampaio M, Calinas F. Gynecological history up to diagnosis and pregnancy outcomes in diagnosed Wilson's disease under therapy-a bicentric matched control cohort study. Rev Esp Enferm Dig 2022;114(4):198–203.
[6] Liu M, Wu K, Wu Y. The emerging role of ferroptosis in female reproductive disorders. Biomed Pharmacother 2023;166:115415.
[7] Guo H, Ouyang Y, Yin H, Cui H, Deng H, Liu H, et al. Induction of autophagy via the ROS-dependent AMPK-mTOR pathway protects copper-induced spermatogenesis disorder. Redox Biol 2022;49:102227.
[8] Sun X, Zhang X, Yan H, Wu H, Cao S, Zhao W, et al. Protective effect of curcumin on hepatolenticular degeneration through copper excretion and inhibition of ferroptosis. Phytomedicine 2023;113:154539.
[9] Dusek P, Hofer T, Alexander J, Roos PM, Aaseth JO. Cerebral iron deposition in neurodegeneration. Biomolecules 2022;12(5):714.
[10] Kalita J, Kumar V, Misra UK, Ranjan A, Khan H, Konwar R. A study of oxidative stress, cytokines and glutamate in Wilson disease and their asymptomatic siblings. J Neuroimmunol 2014;274(1–2):141–8.
[11] Rellmann Y, Eidhof E, Dreier R. Review: ER stress-induced cell death in osteoarthritic cartilage. Cell Signal 2021;78:109880.
[12] Ren J, Bi Y, Sowers JR, Hetz C, Zhang Y. Endoplasmic reticulum stress and unfolded protein response in cardiovascular diseases. Nat Rev Cardiol 2021;18 (7):499–521.
[13] Guzel E, Arlier S, Guzeloglu-Kayisli O, Tabak MS, Ekiz T, Semerci N, et al. Endoplasmic reticulum stress and homeostasis in reproductive physiology and pathology. Int J Mol Sci 2017;18(4):792.
[14] Chen Y, Mi Y, Zhang X, Ma Q, Song Y, Zhang L, et al. Dihydroartemisinin-induced unfolded protein response feedback attenuates ferroptosis via PERK/ATF4/HSPA5 pathway in glioma cells. J Exp Clin Cancer Res 2019; 38(1):402.
[15] Li W, Li W, Leng Y, Xiong Y, Xia Z. Ferroptosis is involved in diabetes myocardial ischemia/reperfusion injury through endoplasmic reticulum stress. DNA Cell Biol 2020;39(2):210–25.
[16] Liao J, Hu Z, Li Q, Li H, Chen W, Huo H, et al. Endoplasmic reticulum stress contributes to copper-induced pyroptosis via regulating the IRE1α-XBP1 pathway in pig jejunal epithelial cells. J Agric Food Chem 2022;70 (4):1293–303.
[17] Wang K, Feng X, Chai L, Cao S, Qiu F. The metabolism of berberine and its contribution to the pharmacological effects. Drug Metab Rev 2017;49 (2):139–57.
[18] Xue W, Xue F, Jia T, Hao A. Research and experimental verification of the molecular mechanism of berberine in improving premature ovarian failure based on network pharmacology. Bioengineered 2022;13(4):9885–900.
[19] Peng Y, Sun L, Guo W, Liu Z, Wang T, Zou T, et al. Berberine protects cyclophosphamide and busulfan-induced premature ovarian insufficiency in mouse model. J Pharmacol Sci 2023;153(1):46–54.
[20] Rondanelli M, Infantino V, Riva A, Petrangolini G, Faliva MA, Peroni G, et al. Polycystic ovary syndrome management: a review of the possible amazing role of berberine. Arch Gynecol Obstet 2020;301(1):53–60.
[21] Di Pierro F, Sultana R, Eusaph AZ, Abrar S, Bugti M, Afridi F, et al. Effect of berberine phytosome on reproductive, dermatologic, and metabolic characteristics in women with polycystic ovary syndrome: a controlled, randomized, multi-centric, open-label clinical trial. Front Pharmacol 2023;14:1269605.
[22] Wang X, Zhang J, Wang S, Song Z, Sun H, Wu F, et al. Berberine modulates gut microbiota to attenuate cerebral ferroptosis induced by ischemia-reperfusion in mice. Eur J Pharmacol 2023;953:175782.
[23] Li X, Chen J, Feng W, Wang C, Chen M, Li Y, et al. Berberine ameliorates iron levels and ferroptosis in the brain of 3 × Tg-AD mice. Phytomedicine 2023;118:154962.
[24] Liang Y, Ye C, Chen Y, Chen Y, Diao S, Huang M. Berberine improves behavioral and cognitive deficits in a mouse model of Alzheimer's disease via regulation of β-amyloid production and endoplasmic reticulum stress. ACS Chem Neurosci 2021;12(11):1894–904.
[25] Wang Y, Wang W, Cheng K, Geng K, Liang J, Wang P, et al. Polycomb subunit Pcgf2 mediates ovulation and fertility through transcriptional regulation progesterone receptor. Front Cell Dev Biol 2022;10:1010601.
[26] Yu J, Zhai D, Hao L, Zhang D, Bai L, Cai Z, et al. Cryptotanshinone reverses reproductive and metabolic disturbances in PCOS model rats via regulating the expression of CYP17 and AR. Evid Based Complement Alternat Med 2014;2014:670743.
[27] Lu J, Xu F, Lu H. LncRNA PVT1 regulates ferroptosis through miR-214-mediated TFR1 and p53. Life Sci 2020;260:118305.
[28] Aguilar Diaz De Leon J, Borges CR. Evaluation of oxidative stress in biological samples using the thiobarbituric acid reactive substances assay. J Vis Exp 2020.
[29] Xie Y, Hou W, Song X, Yu Y, Huang J, Sun X, et al. Ferroptosis: process and function. Cell Death Differ 2016;23(3):369–79.
[30] Doll S, Conrad M. Iron and ferroptosis: a still ill-defined liaison. IUBMB Life 2017;69(6):423–34.
[31] Jiang X, Stockwell BR, Conrad M. Ferroptosis: mechanisms, biology and role in disease. Nat Rev Mol Cell Biol 2021;22(4):266–82.
[32] Tang D, Chen X, Kang R, Kroemer G. Ferroptosis: molecular mechanisms and health implications. Cell Res 2021;31(2):107–25.
[33] Zhao C, Yu D, He Z, Bao L, Feng L, Chen L, et al. Endoplasmic reticulum stress-mediated autophagy activation is involved in cadmium-induced ferroptosis of renal tubular epithelial cells. Free Radic Biol Med 2021;175:236–48.
[34] Song YF, Luo Z, Zhang LH, Hogstrand C, Pan YX. Endoplasmic reticulum stress and disturbed calcium homeostasis are involved in copper-induced alteration in hepatic lipid metabolism in yellow catfish pelteobagrus fulvidraco. Chemosphere 2016;144:2443–53.
[35] Zou L, Cheng G, Xu C, Liu H, Wang Y, Li N, et al. Copper nanoparticles induce oxidative stress via the heme oxygenase 1 signaling pathway in vitro studies. Int J Nanomed 2021;16:1565–73.
[36] Tan Y, Li C, Zhou J, Deng F, Liu Y. Berberine attenuates liver fibrosis by autophagy inhibition triggering apoptosis via the miR-30a-5p/ATG5 axis. Exp Cell Res 2023;427(2):113600.
[37] Jończy A, Lipiński P, Ogórek M, Starzyński RR, Krzysztofik D, Bednarz A, et al. Functional iron deficiency in toxic milk mutant mice (tx-J) despite high hepatic ferroportin: a critical role of decreased GPI-ceruloplasmin expression in liver macrophages. Metallomics 2019;11(6):1079–92.
[38] Li J, Cao F, Yin HL, Huang ZJ, Lin ZT, Mao N, et al. Ferroptosis: past, present and future. Cell Death Dis 2020;11(2):88.
[39] Pan CF, Wei K, Ma ZJ, He YZ, Huang JJ, Guo ZZ, et al. CircP4HB regulates ferroptosis via SLC7A11-mediated glutathione synthesis in lung adenocarcinoma. Transl Lung Cancer Res 2022;11(3):366–80.
[40] Ursini F, Maiorino M. Lipid peroxidation and ferroptosis: the role of GSH and GPx4. Free Radic Biol Med 2020;152:175–85.
[41] Gaschler MM, Stockwell BR. Lipid peroxidation in cell death. Biochem Biophys Res Commun 2017;482(3):419–25.
[42] Xu M, Tao J, Yang Y, Tan S, Liu H, Jiang J, et al. Ferroptosis involves in intestinal epithelial cell death in ulcerative colitis. Cell Death Dis 2020;11(2):86.
[43] Park EJ, Park YJ, Lee SJ, Lee K, Yoon C. Whole cigarette smoke condensates induce ferroptosis in human bronchial epithelial cells. Toxicol Lett 2019;303:55–66.
[44] Zhu Q, Liu Z, Wang Y, Song E, Song Y. Endoplasmic reticulum stress manipulates autophagic response that antagonizes polybrominated diphenyl ethers quinone induced cytotoxicity in microglial BV2 cells. J Hazard Mater 2021;411:124958.